PYRITE OXIDATION RATES FROM HUMIDITY CELL TESTING OF GREENSTONE ROCK[1]

Kim A. Lapakko,[2] and David A. Antonson[2]

Abstract. Fourteen samples of pyrite-bearing Archean greenstone rock (d < 6.35 mm, $0.08 \leq FeS_2 \leq 2.25$ wt. %) were characterized and subjected to laboratory dissolution testing for periods of 154 or 204 weeks. Rates of pyrite oxidation were determined based on the observed rates of sulfate release between weeks 20 and 60 and the calculated pyrite surface areas exposed. The pyrite surface areas exposed were determined based on the particle size distribution, sulfur content of individual size fractions, and percent pyrite liberation. The pyrite oxidation rates, normalized for exposed surface area, ranged from 4×10^{-10} to 18×10^{-10} mol $m^{-2}s^{-1}$ and tended to increase as drainage pH decreased from 7.3 to 3.3. For eight rock samples with median pH values above 6.0, rates were roughly 0.6 to 1.3 times those predicted in the literature for the abiotic oxidation of pyrite by oxygen. Median pH values for the remaining six samples ranged from 3.3 to 5.0, and pyrite oxidation rates were roughly 2 to 8 times the published abiotic rates, suggesting the influence of oxidation by ferric iron.

Additional Key Words: kinetics, kinetic tests, mine waste drainage, drainage quality prediction

---

Introduction

Environmentally sound waste rock management plans are typically required to obtain mineral resource development permits. To develop plans that are effective, efficient, and economical, it is necessary to predict the quality of drainage generated by the lithologies excavated in order to access the ore. Mitigation techniques can then be scaled to the predicted potential for adverse impact. Existing data on a waste rock of composition similar to that at the proposed mine, generated by similar mining methods, and exposed to similar environmental conditions for an extended time provide the best indicator of drainage quality. Since these data are rarely available, it is necessary to use other means of drainage quality prediction, such as compositional characterization and dissolution testing.

Laboratory kinetic tests are commonly conducted to aid in prediction of mine waste drainage quality. Although leachate chemistry and rates of chemical release are typically reported for these tests, rates of mineral dissolution are rarely reported. Whereas dissolution rates have been determined based on laboratory studies conducted on individual, isolated minerals that might be present in a given lithology (e.g. Williamson and Rimstidt, 1994; White and Brantley, 1995), empirical data are needed to provide rates describing their dissolution within a specific rock matrix. Distinct to each lithology are the chemistry, grain size, surface morphology, and extent of exposure (extent to which a mineral grain is exposed to gaseous and aqueous phase reactants) of the individual minerals. Within each lithology the interaction with other minerals and their dissolution products will also be unique. Consequently, it is unknown how well mineral dissolution rates determined from laboratory studies on individual, isolated minerals will approximate rates occurring during mine waste dissolution in the laboratory or field.

Mineral dissolution rates can be helpful when interpreting kinetic test data and in extrapolating predictive test results to full-scale operations. Furthermore, determination of these rates will allow results from dissolution tests on different mineral assemblages to be compiled and compared. This will provide a source of data for a wide variety of mineral assemblages, provide greater insight into factors controlling mine waste weathering, and add a greater degree of confidence to interpretation and extrapolation of kinetic test results. On a practical level, this will reduce uncertainty in mine waste drainage quality predictions.

This paper presents calculates rates of pyrite oxidation during laboratory dissolution testing of Archean greenstone rock from northeastern Minnesota and compares them to those reported in the literature. Greenstones are a mineral exploration target in Minnesota and are host to numerous gold and base metal deposits, although the exact mineralogy and petrology can vary within and among formations. Lapakko and Antonson (2001, 2002) reported on earlier phases of the laboratory studies presented.

Pyrite Oxidation Rates

The major water quality concern regarding mine waste drainage quality is generation of acidic drainage and associated metal leaching, although release of metals in neutral drainage can also adversely impact water quality. Acid is released as a result of the oxidation of iron sulfide minerals (equation 1), which are common in both hydrothermal-quartz-carbonate Au deposits and base metal deposits in greenstones.

$$FeS_2 \; (s) + (15/4) \; O_2 + (5/2) \; H_2O = FeOOH(s) + 2SO_4^{-2} \; (aq) + 4H^+ \; (aq) \tag{1}$$

Williamson and Rimstidt (1994) used literature data (Smith and Shumate, 1970; McKibben, 1984; Nicholson et al., 1988; Moses and Herman, 1991) to derive the following rate law for the abiotic rate of pyrite oxidation by oxygen at 25 ^{o}C.

$$dFeS_2/dt = 10^{-8.19\,(\pm 0.10)}\, m_{DO}^{0.5\,(\pm 0.04)} m_{H+}^{(-0.11\pm 0.01)} \qquad (2)$$

where, m_{DO} and m_{H+} are molalities of dissolved oxygen and H^+ in units of mol kg^{-1}, and where the rate of pyrite destruction is expressed in mol m^{-2} s^{-1}. Ranges of m_{DO} and pH for which the expression is applicable are approximately $10^{-5.5}$ to $10^{-1.5}$ mol kg^{-1} and 2 to 10, respectively. For oxygen saturation at 25 ^{o}C (2.625×10^{-4} mol kg^{-1}) at pH 3 and pH 7, this yields respective rates of 2.2×10^{-10} and 6.2×10^{-10} mol m^{-2} s^{-1}.

In the environment, the rate of sulfide mineral oxidation increases as pH decreases into a range conducive to bacterial mediation of ferrous iron oxidation. Nordstrom (1982) reported that as "pH decreases to 4.5, Fe^{+3} iron becomes more soluble and begins to act as an oxidizing agent." As pH further decreases, bacterial oxidation of ferrous iron becomes the rate limiting step in the oxidation of pyrite by Fe^{+3} iron (Singer and Stumm, 1970), which is the only significant oxidizing agent in this pH range (Nordstrom, 1982; Singer and Stumm, 1970; Kleinmann et al., 1981). The bacterially mediated rate of pyrite oxidation by Fe^{+3} iron is roughly two to three orders of magnitude faster than the rate of abiotic oxidation by O_2 at pH 2 (Nordstrom and Alpers, 1999). In laboratory experiments conducted on hydrothermal quartz carbonate tailings (Lapakko and Wessels, 1995), the SO_4^{-2} release rate from pyrite in the pH range of 3.0 to 3.2 was approximately 13 times that at pH 8 (MN DNR, 2000).

Methods

Materials

As part of a project unrelated to mining, the University of Minnesota Department of Physics constructed a cavern at a depth of 730 m in a greenstone formation near Soudan, MN. The goal of the project was to enlarge an underground physics laboratory at the Soudan Mine, and resulted in excavation of approximately 22,000 cubic yards of greenstone rock. Prior to excavation a 6.35-cm drill hole was bored through the center of the proposed cavern to characterize geotechnical properties of the rock. Because there were also concerns regarding disposal of the rock, drill core intervals were also analyzed for S content using a LECO furnace.

Fourteen samples spanning a range of S contents were collected from the core for laboratory dissolution testing. Five-foot intervals of quarter core were stage-crushed to minus 0.64-cm to limit generation of fines. The three crushing steps were a large jaw crusher set at 1.92 cm, a small jaw crusher set at 0.95 cm, and a roll crusher set at 0.64 cm. After each step the minus 0.64 cm fraction was retained and the plus 0.64 cm fraction was subjected to the next step.

Laboratory Procedures

Fourteen samples of five-cm drill core were stage crushed and subjected to laboratory dissolution testing for 204 weeks. The experimental apparatus was similar to that specified in ASTM Method 5744 (ASTM, 2000) and is described by Lapakko and White (2000). It had a 10.2-cm internal diameter and was approximately 19 cm tall. Each cell was charged with 1000 g of air-dried rock. A total of 18 cells were used for the fourteen drill core samples, four of which were run in duplicate. Prior to sample addition, the cells were washed with 10 % HNO$_3$, and then rinsed three times with distilled water.

Each cell and the contained 1000 g dry solids was weighed, and the solids were then rinsed daily with 500 mL of deionized water for three days (week 0) to remove oxidation products which accumulated prior to the beginning of the experiment. The outlet port was capped and 500 mL of deionized water was added slowly from a graduated cylinder to the cell. Ten minutes after all cells were filled, the outlets were uncapped and the cells drained. Subsequently the cells were rinsed weekly in a similar manner, with the exception that a single 500-mL volume of deionized water was slowly dripped into the cell from a separatory funnel. Dissolution tests on twelve solids continued for 204 weeks. The four replicates of these samples and two additional samples were terminated after 154 weeks of dissolution.

Between rinses, the cells were stored in a room in which temperature and humidity were controlled. Over the 204-week period of testing, temperature and relative humidity were measured three to four times per week, and average weekly values were determined. Temperature ranged from 22.2 $^{\circ}$C to 27.5 $^{\circ}$C and averaged 24.5 $^{\circ}$C, with a standard deviation of 1.1 $^{\circ}$C. Average weekly relative humidity ranged from 51.3% to 63.5% and averaged 57.9%, with a standard deviation of 2.4%.

Analyses

Particle size distribution for the laboratory samples was determined using method ASTM E-276-93 (ASTM, 2000) by Lerch Brothers Inc. All samples were dry-sieved and two samples were also wet-sieved.

The rock samples, as well as their size fractions, were analyzed for S, SO_4^{-2} (sulfide was determined by difference), and evolved CO_2 by ACTLABS in Tucson, AZ using ASTM E-1915-97 (ASTM, 2000). A 10 % HCl solution was used to decompose the carbonate minerals, and the carbonate present was quantified as the difference between total carbon in the initial sample and that in the residue. The remaining solid-phase constituents of the bulk samples were determined by ACTLABS in Ancaster, ON. Whole rock constituents were determined using a lithium tetraborate fusion modified from ASTM E-886-94 (ASTM, 2000) and analysis by inductively coupled plasma-atomic emission spectroscopy (ICP-AES) using a Thermo Jarrell-Ash ENVIRO II ICP. Concentrations of Ag, Cd, Cu, Ni, Pb, Zn, and Bi were determined using a total digestion method modified from Crock et al. (1983), with analysis by ICP-AES. Other trace elements were determined using instrumental neutron activation analysis (Hoffman, 1992). Mineral content was determined using sample chemistry, optical microscopy, and previous x-ray diffraction data on drill core samples. Chemistry of the siderite present in two of the samples was determined by scanning electron microscope (Zeiss DSM 960A) using electron dispersive spectrometry.

Pyrite oxidation rates were calculated based on the pyrite surface area that would be exposed to gaseous and aqueous phase reactants in dissolution tests. The extent of pyrite liberation, the degree to which pyrite grains are separated from the rock matrix, was determined microscopically by loose grain counts of particles in 11 or 12 size fractions (Louis Mattson, Mineralogical Consulting Service, Pengilly, MN). It was assumed that the surface area of the liberated pyrite contributed virtually all of the exposed pyrite surface area (i.e. pyrite area exposed on rock surfaces was negligible).

Water samples were analyzed for specific conductance, pH, alkalinity, and acidity at the Minnesota Department of Natural Resources laboratory in Hibbing, MN. Specific conductance was determined using a Myron L conductivity meter. An Orion SA720 meter, equipped with a

Ross combination pH electrode (8165), was used for pH determinations. Alkalinity (for pH ∃ 6.3) and acidity were determined using standard titration techniques for endpoints of 4.5 and 8.3, respectively (American Public Health Association et al., 1992). Samples were filtered through a 0.45-micron filter for sulfate determinations using a Lachat QuickChem 8000 or, for $[SO_4^{-2}]$ < 5 mg/L, a Dionex ion chromatograph at the MN Department of Agriculture. Concentrations of other solutes were also determined, but those results are not immediately relevant to the present paper.

Calculations

Rates of pyrite oxidation were determined by dividing molar rates of SO_4^{-2} release by twice the liberated pyrite surface area. The division by two accounts for the fact that there are two moles of SO_4^{-2} released per mole of pyrite oxidized. Sulfate release rates were determined for periods 20-60, 60-100, 100-154, and 154-204 weeks. The rates for a specific period were calculated as the average of the weekly SO_4^{-2} release rates during the period. An average rate of release for weeks 20-204 was calculated as the total SO_4^{-2} mass released during this time divided by 185.

The exposed pyrite surface area of a sample was determined by summing the exposed pyrite surface area in each particle size fraction, which was calculated as follows.

$$A_{py, i} = (\%S^{2-}_i/100)[(55.85 + 64.12)/64.12][6/(\rho\, d_{gm, i})]M_i L_i (SR)/100, \text{ where} \qquad (3)$$

$A_{py, i}$ = pyrite area in particle size fraction i, m^2,

$\%S^{-2}_i$ = percent sulfide (S^{-2}) of sample in size fraction i,

ρ = pyrite density = 5.02×10^6 g m^{-3},

$d_{gm, i}$ = geometric mean diameter of particle size fraction i, m,

M_i = mass of rock in particle size fraction i, g,

L_i = percent pyrite exposure in particle size fraction i, and

SR = surface roughness factor for pyrite estimated as 2.6, using the value reported for quartz (Parks, 1990) because pyrite surfaces were reported to be smooth.

The mass weighted sulfide concentrations for the individual size fractions were compared to the sulfide content of the bulk sample. The agreement between the two values was reasonable. A minimum diameter of 10 μm was used to determine the geometric mean diameter of the less than 75-μm fraction. The mineralogical analysis indicated the pyrite finer than 10 μm was "intergrown with the gangue minerals" (Mattson, 2000), which limited the pyrite surface exposure.

All laboratory samples were dry sieved and two samples were wet sieved. The mass in the wet-sieved 10-75 μm fraction averaged 1.26 times the dry-sieved fraction. The influence of wet sieving on other size fractions was negligible. Consequently, the 10-75 μm fraction mass of dry-sieved samples was multiplied by this factor.

Results and Discussion

Rock Composition

The 14 greenstone samples were analyzed for particle size distribution, chemistry, and mineralogy. Solids were crushed to finer than 6.4 cm. Approximately 23 to 35 percent of the particles were finer than 850 μm, 9 to 14 percent finer than 212 μm, and 5 to 8 percent finer than 75 μm (Table A1). Sulfur contents of the 14 samples ranged from 0.04 to 1.22 percent, and the sulfate-sulfur content exceeded 0.016% in only one sample (Table 1).

Quartz (24-77%), chlorite (10-55%), and sericite (5-42%) contributed 90 to 98 weight percent of the mineral content in 13 of the 14 samples (Table 1). The exception was the 0.72%-S sample, in which the contribution of these three minerals was 77 percent and siderite $(Fe_{1.79}Mn_{0.15}Mg_{0.13}Ca_{0.003}Na_{0.07}(CO_3)_2)$ content was 17.9 percent. Appreciable siderite $(Fe_{1.74}Mn_{0.13}Mg_{0.18}Ca_{0.004}Na_{0.06}(CO_3)_2)$ was also present in the 0.50%-S sample, contributing 4.6 weight percent of the sample mass.

Table 1. Summary of sample compositions. Values in weight percent.

%S	%SO$_4$-S	CO$_2$	Pyrite	Quartz	Chlorite	Sericite	Siderite
0.04	<0.016	<0.05	0.1	29	55	12	<0.1
0.05a	<0.016	<0.05	0.1	24	30	42	<0.1
0.05b	<0.016	<0.05	0.1	24	39	32	<0.1
0.10	<0.016	<0.05	0.2	56	26	13	<0.1
0.12	<0.016	<0.05	0.2	28	41	28	<0.1
0.16a	<0.016	<0.05	0.3	48	31	13	<0.1
0.16b	<0.016	<0.05	0.3	42	35	19	<0.1
0.20	<0.016	0.05	0.4	72	14	12	0.1
0.26	<0.016	<0.05	0.5	68	14	8	<0.1
0.39	0.016	<0.05	0.7	59	21	16	<0.1
0.50	0.033	1.76	0.9	59	12	21	4.6
0.59	<0.016	<0.05	1.1	77	10	5	<0.1
0.72	<0.016	6.85	1.4	51	12	14	17.9
1.22	0.016	<0.05	2.2	48	33	13	<0.1

Pyrite was the only sulfide mineral reported, in quantities of 0.1 to 2.2 percent. Based on the overall mineralogy and chemistry, the small amounts of SO_4^{-2} were assumed to be present as melanterite, with contents not exceeding 0.3 percent (Mattson, 2000). Pyrite grains ranged from coarse (600 μm) "to very fine (<10 μm) grains intergrown with the gangue minerals." The distribution of pyrite grain sizes was fairly constant among the samples. Pyrite content, as inferred by sulfur content, tended to increase as particle size decreased (Table A2). Pyrite liberation in the !300 μm or !200 μm fractions was generally greater than 50 percent, with little liberation in the coarser fractions (Mattson, 2000). The extent of liberation increased as particle size decreased below 300 μm, and was generally greater than or equal to 90 percent for particles less than 106 μm in diameter (Table A3).

Drainage Volume and Water Retention

Each week 500 mL of water was added to each cell. For each sample, the mass of water retained after this addition was fairly stable over the course of the experiment and decreased only slightly during the weekly cycle. One day after the addition the mean water retention in 12 of the solids ranged from 129 to 153 mL, indicating typical water retentions of 13 to 15 percent of the solids weight. Mean water retention for the 0.72% S and 0.26% S solids averaged 111 and 163 mL, respectively. Based on the percentage of mass in the −850-μm fraction, the 0.72% S sample was the coarsest of the solids tested and the 0.26% S sample was the finest (Table A1). This suggests, quite reasonably, that the water retention was a function of particle size distribution. The water retention for each cell was fairly consistent, and the standard deviations for the 14 samples ranged from three to eight percent of the mean value. The mean water retention prior to water addition indicated that, on average, the cells lost two to ten mL of water to evaporation during the weekly cycle (Table A4).

One implication of the water retention values is that the finer particles in the cells were very likely water saturated. These particles have a relatively high specific surface area and are, therefore, more reactive per unit mass. The pyrite in the finer fractions is also more likely to be liberated from the rock matrix and, therefore, exposed for reaction.

Sulfate Release Rates

The replication of both drainage pH and sulfate release rates was excellent. For each of the four pairs of duplicate samples, drainage pH and SO_4^{-2} release rates were determined for three different rate periods (20-60, 60-100, 100-154 weeks) over a period of roughly 2.5 years. For the twelve comparative sets of data, median drainage pH values differed by no more than 0.07 units, and the difference from the mean for SO_4^{-2} release rates was less than five percent (Table 2).

Variation of SO_4^{-2} release rates within a rate period was generally within about 25 percent of the mean value. Sulfate release rates were calculated as the mean of the weekly rates during the specified period. The standard deviation for each period was also calculated to provide a measure of variability within the rate period. The standard deviations ranged from 0.04 to 0.35 times the mean rate, although the typical range for this fraction was roughly 0.08 to 0.25 (Table 2).

Sulfate release rates tended to increase with increasing S content. This trend was observed for all rate periods and was depicted by plotting the SO_4^{-2} release rate after week 20 as a function of S content to provide an overview of the entire data set (Fig. 1). Data from samples generating high drainage pH values tended to fall below the regression line, and the opposite trend was observed for samples generating low drainage pH.

As S content increased, drainage pH tended to decrease (Table 2). However, the 0.50%-S and 0.72%-S solids produced higher drainage pH than would be expected based on the general relationship between S content and drainage pH. Dissolution of the $MgCO_3$ fraction of the siderite present in these samples neutralized much or all of the acid produced as a result of pyrite oxidation, thus elevating drainage pH. Despite their higher S contents, the SO_4^{-2} releases per unit exposed pyrite area from these samples were consistent with those of the lower S content samples that generated relatively high pH. This further demonstrates that pH, in addition to pyrite surface area, influences rates of SO_4^{-2} release.

Table 2. Observed sulfate release rates in $\mu mol \ (kg \ rock)^{-1}wk^{-1}$.

%S	Weeks 20-60			Weeks 60-100			Weeks 100-154			Weeks 154-204			$Rate_{final}/Rate_{initial}$
	pH_{med}	dSO$_4$/dt		pH_{med}	dSO$_4$/dt		pH_{med}	dSO$_4$/dt		pH_{med}	dSO$_4$/dt		
		rate	s.d.		rate	s.d.		rate	s.d.		rate	s.d.	
0.04	7.26	4.98	0.91	7.04	4.46	0.74	7.12	3.94	0.39	7.01	3.16	0.26	0.63
0.05a[1]	7.05	7.81	1.26	6.88	6.57	1.29	6.69	4.89	0.60	6.58	3.88	0.30	0.50
0.05b[1]	7.05	5.42	1.19	6.87	4.87	0.91	6.72	4.30	0.62	6.56	4.09	1.2	0.75
0.10 rep 1	6.74	13.0	1.70	6.37	11.7	1.36	6.00	9.58	1.7	5.90	6.92	1.6	0.53
0.10 rep 2	6.69	13.6	1.11	6.31	11.6	1.37	6.06	10.5	1.4	Ended week 154			0.77
0.12	6.66	15.7	2.45	6.33	10.7	1.84	6.18	8.38	1.7	6.02	6.91	0.45	0.44
0.16a[1]	6.76	20.3	2.23	6.34	19.4	2.65	6.15	17.1	4.3	5.91	13.8	0.51	0.68
0.16b[1] rep 1	6.38	18.2	2.39	6.06	15.0	2.15	5.78	13.4	2.9	5.61	10.8	0.68	0.59
0.16b[1] rep 2	6.43	18.3	2.05	5.99	15.9	2.85	5.82	13.3	2.9	Ended week 154			0.73
0.20	4.54	58.8	10.6	4.15	66.6	9.91	4.13	58.4	15.0	4.10	46.2	3.4	0.79
0.26	4.78	85.4	11.6	3.95	90.8	7.14	3.87	94.7	18.0	Ended week 154			1.10
0.39	4.35	103	21.5	3.97	120	28.5	3.96	110	38.0	Ended week 154			1.07
0.50	5.04	186	41.7	5.63	116	16.5	6.47	92.5	22.1	6.88	69.3	5.2	0.37
0.59 rep 1	3.33	361	61.9	3.29	311	34.3	3.36	280	74.0	3.45	195	17.6	0.54
0.59 rep 2	3.29	379	70.4	3.27	331	46.5	3.35	293	79.0	Ended week 154			0.77
0.72	7.16	106	22.1	7.68	98.3	28.1	7.84	89.9	15.0	7.81	99.4	12.4	0.94
1.22 rep 1	3.67	244	46.5	3.51	300	66.6	3.55	301	83.0	Ended week 154			1.23
1.22 rep 2	3.63	266	44.5	3.47	305	34.0	3.50	289	29.0	3.50	274	22.6	1.03

1   Sulfur contents followed by "a" and "b" signify two different samples.

As would be expected, SO_4^{-2} release rates tended to decrease with time, and rates during weeks 154-204 were typically 50 to 80 percent of those during weeks 20-60 (Table 2). Pyrite depletion and development of Fe oxyhydroxide coatings on the pyrite surfaces may have contributed to decreasing release rates. The extent of pyrite depletion, as indicated by SO_4^{-2} release, typically ranged from 5 to 9% for samples with median pH values of at least 4.18 and 15 to 30% for lower pH samples (Table A5). Samples with S contents of 0.26, 0.39, 0.72, and 1.22 percent did produce final rates that were near or above those generated initially, although the period of record for the first two samples was limited to 154 weeks.
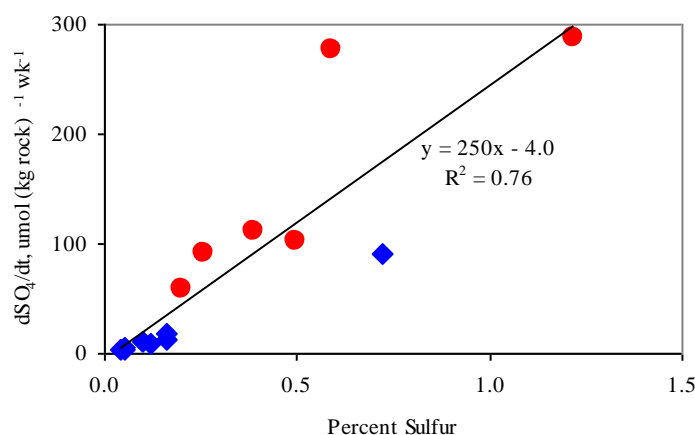
Figure 1. Average SO_4^{-2} release rates after week 20 tended to increase with increasing s content. Samples generating high pH (blue diamonds represent median pH values above 6) tended to fall below the regression line, and those generating low pH (red circles represent median pH values below 6) tended to fall above the regression line.

Pyrite Oxidation Rates

Sulfate release rates and estimated exposed pyrite surface areas were used to determine normalized oxidation rates for pyrite in the samples. It was assumed that 1) all SO_4^{-2} release was due to oxidation of pyrite (the only sulfide mineral reported present), 2) all SO_4^{-2} released by pyrite oxidation was transported with the drainage, and 3) only exposed pyrite surfaces oxidized and this exposure was approximated by that of liberated pyrite grains (i.e. oxidation of interstitial or included pyrite was negligible).

With regard to the first assumption, it should be noted that small amounts of SO_4^{-2} were present in the rock, and it was assumed to be present as melanterite (see previous section on rock composition). It was assumed that any melanterite, or other soluble SO_4^{-2} minerals, was removed with the three rinses prior to experimentation and within the first few weeks of the experiment. Rates presented in this paper reflect drainage quality after week 20, well beyond the expected period of melanterite dissolution. With regard to the second assumption, chemical precipitation or inefficient rinsing of soluble reaction products can limit transport. Chemical precipitation is unlikely because Ca concentrations were low, and SO_4^{-2} concentrations were more than two orders of magnitude below gypsum saturation. The rinsing efficiency was likely quite high since the weekly rinse volume was in excess of two pore volumes and the rinse water was allowed to remain in contact with the solids for at least ten minutes.

Two approaches were used to determine pyrite oxidation rates, and both used the exposed pyrite surface area determined based on the solid-phase analyses. However, different periods for SO_4^{-2} release and methods of data analysis were applied. In the first approach, the SO_4^{-2} release observed for weeks 20-204 (or 20-154 for the 0.20%-S and 0.26%-S samples) was used. For replicated samples, only the cell with the longer period of record was used. Thus, the data used included roughly 90 percent of the three- to four-year period of record for 14 samples. It should be noted, however, that this assessment ignores changes in drainage pH and SO_4^{-2} release rates over time and is intended as an initial estimation of the pyrite oxidation rates.   These data were

analyzed by regressing half the rate of SO_4^{-2} release against the exposed pyrite surface area (Table A5). The SO_4^{-2} release rate was multiplied by 0.5 to account for the fact that one mole of SO_4^{-2} release implies oxidation of one half mole pyrite (FeS_2).

As indicated in Fig. 1, SO_4^{-2} release rates were related to drainage pH. Based on inspection of data, the regression was conducted for rates with median drainage pH from 4.02 to 7.67 (Fig. 2). For this pH regime, the regression yielded a pyrite oxidation rate of 6.9×10^{-10} mol $m^{-2}s^{-1}$ ($r^2 = 0.85$ and $n = 12$). Inserting these pH values and a dissolved oxygen concentration of 2.6×10^{-4} mol kg^{-1} into equation 2 (Williamson and Rimstidt, 1994) yields respective predicted rates of 2.9×10^{-10} and 7.3×10^{-10} mol $m^{-2}s^{-1}$ for the abiotic oxidation of pyrite by O_2. Thus, the pyrite oxidation rate determined using average SO_4^{-2} release rates observed after week 20 for median pH values of 4.02 to 7.67 was at the upper end of the predicted range. This is consistent with the abiotic oxidation of pyrite by O_2.
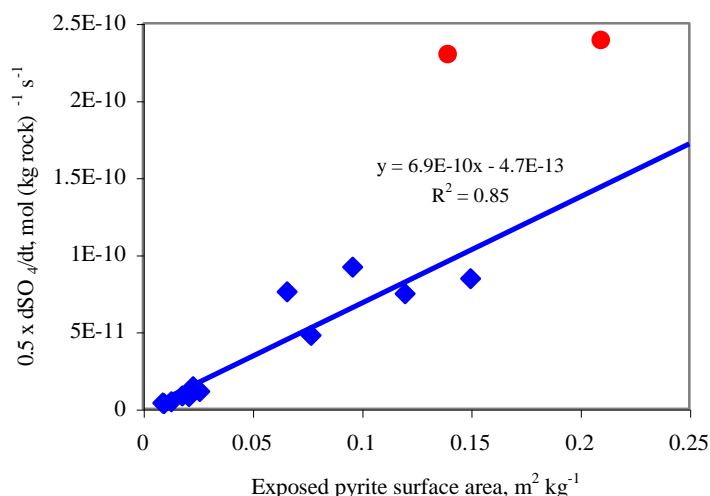

Figure 2. Average SO_4^{-2} release rates after week 20 were regressed against exposed pyrite surface areas to obtain pyrite oxidation rates. The twelve blue diamonds and solid line represent samples with median pH values of 4.18 to 7.67. The red circles represent samples with median pH values of 3.35 and 3.53 and were not included in the regression.

For the remaining two samples, the median pH values were 3.35 and 3.53. The observed SO_4^{-2} release rates at these pH values were roughly twice those predicted based on the linear regression analysis (Table A5). Although this is not a large difference, it suggests that mechanisms other than abiotic oxidation by O_2, most likely reaction with Fe^{+3} iron, may have influenced pyrite oxidation. Nordstrom (1982) indicated this reaction becomes more dominant as pH decreases below 4.5, although the results in Fig. 2 suggest a threshold value in the neighborhood of pH 3.5 for the pyrite present in the greenstone rock.

In the second approach, pyrite oxidation rates were calculated for all 14 individual samples and four replicates during weeks 20-60. Rates for weeks 20-60 were selected as the most appropriate for presentation because effects of Fe oxyhydroxide coating on pyrite mineral surfaces would be minimized. The rates determined ranged from roughly 4×10^{-10} to

18×10^{-10} mol m^{-2}s^{-1} (Table 3). The calculated rates increased slightly with decreasing pH, and for median drainage pH ranges above 3.5 (observed range of 3.63 to 7.26 for 13 samples) the maximum rate was roughly 2.5 times the minimum rate. The 0.59 %S samples generated median pH values near 3.3 and the calculated pyrite oxidation rates were roughly four times the minimum observed. The logarithm of rates was plotted against pH, with data from duplicated samples averaged. Regression analysis yielded a slope of –0.1 for the 14 samples ($r^2 = 0.68$) (Fig. 3). This slope indicates that the variation of calculated pyrite oxidation rates with drainage pH was relatively small.

Table 3. Comparison of pyrite oxidation rates observed in the laboratory during weeks 20-60 to those predicted by Williamson and Rimstidt (1994).

% S	pH_{med}	Sulfate release rate, weeks 20-60 μmol (kg rock)$^{-1}$wk^{-1}		Exposed FeS_2 surface area, m^2 kg^{-1}	$dFeS_2/dt$, mol m^{-2} s^{-1} $\times 10^{-10}$		$dFeS_2/dt$, obs/ pred
		Rate	s.d.		Obs.	Pred[3]	
0.04	7.26	4.98	0.91	0.0096	4.3	6.6	0.65
0.05a[1]	7.05	7.81	1.26	0.013	5.0	6.2	0.80
0.05b[1]	7.05	5.42	1.19	0.0090	5.0	6.2	0.80
0.10 rep 1	6.74	13.0	1.70	0.018	6.0	5.8	1.04
0.10 rep 2[2]	6.69	13.6	1.11	0.018	6.2	5.7	1.10
0.12	6.66	15.7	2.45	0.021	6.2	5.7	1.09
0.16a[1]	6.76	20.3	2.23	0.023	7.3	5.8	1.26
0.16b[1] rep 1	6.38	18.2	2.39	0.026	5.8	5.3	1.10
0.16b[1] rep 2[2]	6.43	18.3	2.05	0.026	5.8	5.3	1.09
0.20	4.54	58.8	10.6	0.077	6.3	3.3	1.91
0.26[2]	4.78	85.4	11.6	0.066	10.7	3.5	3.05
0.39[2]	4.35	103	21.5	0.096	8.9	3.1	2.82
0.50	5.04	186	41.7	0.14	10.3	3.7	2.74
0.59 rep 1	3.33	361	61.9	0.17	17.6	2.4	7.22
0.59 rep 2[2]	3.29	379	70.4	0.17	18.4	2.4	7.66
0.72	7.16	106	22.1	0.12	7.3	6.4	1.14
1.22 rep 1	3.67	244	46.5	0.21	9.6	2.7	3.63
1.22 rep 2	3.63	266	44.5	0.21	10.5	2.6	3.99

[1] Sulfur contents followed by "a" and "b" signify two different samples.
[2] Terminated at week 154 and sulfate release rates are for weeks 100-154.
[3] Predicted rates based on Williamson and Rimstidt (1994) = dFeS/dt = $10^{-8.19\,(\pm0.10)}m_{DO}{}^{0.5(\pm0.04)}m_{H+}{}^{(-0.11\,\pm0.01)}$; $m_{DO}=2.625\times10^{-4}$, assuming O_2 saturation at 25 °C.
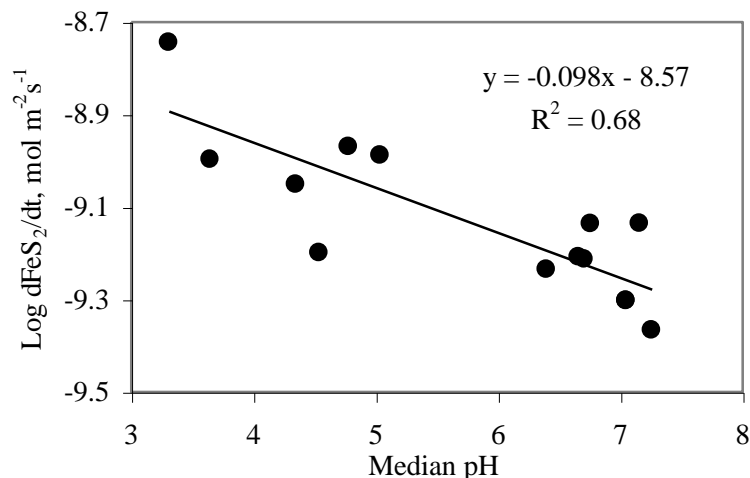
Figure 3. Pyrite oxidation rates for weeks 20-60 increased with decreasing median drainage pH. Values for duplicate cells were averaged.

These individual rates were compared with rates predicted by Williamson and Rimstidt (1994) for abiotic oxidation of pyrite by O_2. The predicted rates were determined using the median pH of drainage from the sample during the rate period. The pyrite oxidation rates calculated for greenstone samples ranged from 0.65 to 7.7 times those predicted, and the ratio of the calculated rates to those predicted increased with decreasing pH (Table 3). The latter trend is not surprising given the observed rates increased slightly with decreasing pH (Fig. 3) and equation 2 predicts that rates decrease with decreasing pH.

For the eight samples (ten cells) with median drainage pH greater than or equal to 6.0, the ratio of observed to predicted rates ranged from 0.65 to 1.26, indicating that the observed rates were 65 to 126 percent of those predicted (Table 3). Thus, for drainage pH > 6 the observed rates were in close agreement with those predicted by Williamson and Rimstidt (1994). They were roughly twice the average weekly rate derived from the expression presented by Jerz and Rimstidt (2004). Given the fact that most of the exposed pyrite occurred in fine-grained particles that were in a water-saturated state, a condition that might occur in waste rock piles, the reaction conditions in the present experiment were markedly different than those employed to examine pyrite oxidation in moist air. For the six samples (eight cells) with median drainage pH values from 3.3 to 5.0 the ratio of observed rates to those predicted by Williamson and Rimstidt (1994) ranged from 1.9 to 7.7 (Table 3).

The increase in calculated pyrite oxidation rates with decreasing pH (Fig. 3) suggests that oxidation by Fe^{+3} iron might have become more influential as pH decreased, particularly as pH decreased below 3.5, a value consistent with that indicated by Fig. 2. The extent of oxidation by Fe^{+3} iron does not appear to be great. Although rates increased at low pH, they appear to be substantially lower than the rate predicted for abiotic oxidation of pyrite by Fe^{+3} iron by Williamson and Rimstidt (1994). It is possible that the retention time in the cells was inadequate for substantial oxidation of Fe^{+2} iron to occur, especially if bacterial mediation of this reaction was small.

It is also possible that the specific surface area of pyrite increased as sulfur content increased. This could occur if pyrite surfaces in the higher S solids were rougher or if characteristic pyrite grain size in the –75 μm fraction decreased as S content increased. This would yield a larger pyrite surface area as S content increased which would, in turn, lead to more rapid SO_4^{-2} release. However, the pyrite oxidation rate determined for the 0.72%-S sample was consistent with that observed for the lower-sulfur solids, all of which generated drainage pH values above 6.0. This suggests that the increase in oxidation rates at low pH was due to mechanisms other than the abiotic reaction of pyrite and O_2.

Assessment of Calculated Rates

The pyrite oxidation rates calculated for the greenstone samples were based on determinations of S content, particle size distribution, degree of pyrite liberation, a surface roughness factor for the pyrite present, and the observed rate of SO_4^{-2} release with humidity cell drainage. The agreement between the mass-weighted S content determined from the various size fractions and the bulk sample S content suggests the S determinations did not introduce substantial error. Rates were calculated based on the analyses of the size fractions, and the mass-weighted mean S contents were generally 0.8 to 1 times the bulk S contents (Table A2). A 20 percent underestimation of S content in the finest fractions would result in a 25 percent overestimation of the pyrite oxidation rate.

The particle size distribution was determined by dry sieving and was shown to be subject to error. Two samples were wet sieved and the pyrite surface area calculated was roughly 26 percent higher than that determined by dry sieving, due to the increased mass of the –75 μm fraction with wet sieving. The wet-sieved data were believed to be more accurate, and the dry-sieved –75 μm fractions were multiplied by 1.26 to account for the difference in methods. Nonetheless, more rigorous determination of the wet-sieved particle size distribution would be beneficial. Furthermore, the calculation is sensitive to the minimum pyrite diameter. A minimum diameter of 10 μm was selected based on the observation that finer grains were intergrown with gangue minerals (Mattson, 2000). Changing the minimum diameter to 5 μm would increase the calculated pyrite surface area of the 10-75 μm fraction and decrease the calculated pyrite oxidation rate by roughly 40 percent.

Although error introduced by pyrite liberation assessments are believed to be small the surface roughness factor of the pyrite present was not determined directly. A value of 2.6 was used for calculations and is at the lower end of the range of surface roughness factors reported for pyrite. For example, surface roughness factors of 2.4, 3.7, 5.2, 5.5, and 7.6 were calculated from data presented by Moses and Herman (1991), McKibben and Barnes (1986), Kamei and Ohmoto (2000), Jantzen et al. (1997), and Williamson and Rimstidt (1994), respectively. The use of a roughness factor of 7.6 would have resulted in rates roughly one-third of those determined. However, all of these studies determined BET surface areas on pyrite that had been crushed or ground. Drill core samples in the present study were subjected to crushing using jaw crushers set at 1.92 and 0.95 cm and a roll crusher set at 0.64 cm. Relative to directly crushing pyrite, this method of size reduction most likely had minimal impact on the surface of pyrite grains that were less than 600 μm in diameter. Consequently, it is believed that the surfaces would tend to be smoother than those subjected to more rigorous crushing and grinding and, therefore, a surface roughness factor at the lower end of the range was appropriate.

In contrast to exposed pyrite surface area determinations, error introduced by the SO_4^{-2} release rates used to calculate pyrite oxidation rates was likely small. Each of these rates was

based on at least ten measurements, and the standard deviations determined indicate that variation within rate periods was not excessive. Furthermore, sulfate release rates from four sets of duplicate samples replicated very well over the course of the experiment.

Thus, most of the uncertainty in the calculated rates of pyrite present in greenstone rock samples was related to determination of surface area. Although care was taken to ensure the error introduced by solid phase analyses was relatively small, additional work could be conducted to reduce uncertainty in the calculations. Wet-sieving existing splits sample would increase the accuracy of the particle size distribution, particularly the fine size fractions in which pyrite is largely liberated. Additional detailed examination of grain size and surface roughness of pyrite present in the fine fractions would provide a check on the initial analysis. Direct determination of the specific surface area of pyrite would further increase the integrity of the data.

Conclusions

Laboratory dissolution studies were conducted on well-characterized Archean greenstone rock in which pyrite was the only sulfide mineral identified. The exposed pyrite surface area was calculated for samples tested based on particle size distribution and S content and degree of pyrite liberation in individual size fractions. Rates of pyrite oxidation were determined based on the exposed pyrite surface area calculated and the SO_4^{-2} release observed in drainage. The laboratory rates calculated for samples generating drainage pH values above six were in close agreement with those predicted for the abiotic oxidation of pyrite by dissolved O_2 (Williamson and Rimstidt, 1994). The calculated oxidation rates increased slightly with decreasing drainage pH and the dependence appeared to increase as drainage pH decreased below 3.5. This suggests mechanisms other than abiotic oxidation by O_2 might be influential at lower pH.

Acknowledgements

Literature Cited

ASTM. 2000. D5744-96, Standard test method for accelerated weathering of solid materials using a modified humidity cell. p. 257-269. *In*: Annual Book of ASTM Standards, 11.04. American Society for Testing and Materials, West Conschohocken, Pennnsylvania.

American Public Health Association (APHA), American Water Works Association, Water Environment Federation. 1992. Standard Methods for the Examination of Water and Wastewater, 18th edition. American Public Health Association, Washington, D.C.

Crock, J. G., Lichte, F. E., and Briggs, P. H. 1983. Determination of elements in National Bureau of Standards' geological reference materials SRM 278 obsidian and SRM 688 basalt by inductively coupled argon plasma-atomic emission spectrometry. Geostandards Newsletter, 7. p. 335-340. http://dx.doi.org/10.1111/j.1751-908X.1983.tb00395.x

Hoffman, E.L. 1992. Instrumental neutron activation in geoanalysis. Jour. Geochem. Explor., 44. p. 297-319. http://dx.doi.org/10.1016/0375-6742(92)90053-B

Janzen, M.P., R.V., Nicholson and J.M. Scharer. 1997. The role of enhanced particle surface area, crystal structure and trace metal content on pyrrhotite oxidation rates in tailings. p. 399-415. *In*: Proceeding of the Fourth International Conference on Acid Rock Drainage. Vol. 1. Vancouver, British Columbia, May 31 - June 6, 1997.

Jerz, J.K. and D.J. Rimstidt. 2004. Pyrite oxidation in moist air. Geochchim. Cosmochim. Acta 68. p. 701-714. http://dx.doi.org/10.1016/S0016-7037(03)00499-X.

Kamei, G., ahd H. Ohmoto. 2000. The kinetics of reactions between pyrite and O2-bearing water revealed from in situ monitoring of DO, Eh, and pH in a closed system. Geochchim. Cosmochim. Acta 64. p. 2585-2601.

Kleinmann, R.L.P., D.A. Crerar and R.R. Pacelli. 1981. Biogeochemistry of acid mine drainage and a method to control acid formation. Mining Eng. March 1981.

Lapakko, K.A. and D.A. Antonson. 2001. Laboratory drainage pH and sulfate release rates from Archean Greenstone rock. p. 384-393. *In*: Securing the Future, International Conference on Mining and the Environment. June 25-July 1, Skellefte□, Sweden.

Lapakko, K.A. and D.A. Antonson. 2002. Drainage pH, acid production, and acid neutralization for Archean greenstone rock. Preprint 02-73. *In*: Proc. 2002 SME Annual Meeting, February 25-27, Phoenix, AZ (CD-ROM). Soc. For Mining, Metallurgy, and Exploration, Inc. Littleton, CO.

Lapakko, K. A., J.N. Wessels. 1995. Release of acid from hydrothermal quartz-carbonate hosted gold-mine tailings. p. 139-148. *In*: Sudbury '95, Conference on Mining and the Environment, Sudbury, Ontario, May 28th - June 1st, 1995.

Lapakko, K.A. and W.W. White III. 2000. Modification of the ASTM D5744-96 kinetic test. p. 631-639. *In*: Proc. from the Fifth International Conference on Acid Rock Drainage. SME, Littleton, CO.

Mattson, L.A. 2000. Soudan mine cavern sample mineralogy. Report to Minnesota Department of Natural Resources from Louis A. Mattson, Mineralogical Consulting Service, Pengilly, MN. 27 September 2000. 6 p.

Mattson, L.A. 2001. Personal communication with Louis A. Mattson, Mineralogical Consulting Service, Pengilly, MN. January 2001.

Minnesota Department of Natural Resources. 2000. Unpublished data for tailings sample T9 in the experiment on dissolution of hydrothermal quartz carbonate gold tailings. Minnesota Department of Natural Resources, Division of Lands and Minerals, St. Paul, MN.

McKibben, M.A. 1984. Kinetics of aqueous oxidation of pyrite by ferric iron, oxygen, and hydrogen peroxide from pH 1-4 and 20-40°C. Ph.D. thesis. Pennsylvania State University.

McKibben, M.A. and J.L Barnes. 1986. Oxidation of pyrite in low temperature acidic solutions: Rate laws and surface textures. Geochim. Cosmochim. Acta 50. p. 1509-1520. http://dx.doi.org/10.1016/0016-7037(86)90325-X.

Moses, C.O. J.S. Herman. 1991. Pyrite oxidation at circumneutral pH. Geochim. Cosmochim. Acta 55. p. 471-482. http://dx.doi.org/10.1016/0016-7037(91)90005-P

Nicholson, R.V., R.W. Gillham and E.J. Reardon. 1988. Pyrite oxidation in carbonate-buffered solution: 1. Experimental kinetics. Geochim. Cosmochim. Acta 52. p. 1077-1085. http://dx.doi.org/10.1016/0016-7037(88)90262-1

Nordstrom, D. K. 1982. Aqueous pyrite oxidation and the consequent formation of secondary iron minerals. p. 37-56. *In*: Acid Sulfate Weathering. K.A. Cedric, D.S. Fanning, and I.R. Hossner (eds.), Soil Sci. Soc. America Spec. Pub. 10.

Nordstrom, D.K. and C.N. Alpers. 1999. Geochemistry of acid mine waters. *In*: The Environmental Geochemistry of Mineral Deposits. Part A: Processes, Techniques, and Health Issues. p. 133-160. Vol. 6A, Ch. 4. Reviews in Economic Geology. Society of Economic Geologists, Inc., Chelsea, MI.

Parks, G.A. 1990. Surface energy and adsorption at mineral-water interfaces: An introduction. Reviews in Mineralogy 23. p. 133-175.

Singer, P.C. and W. Stumm. 1970. Acid mine drainage: The rate determining step. Science, 167. p. 1121-1123. http://dx.doi.org/10.1126/science.167.3921.1121

Smith E.E. and L.S. Shumate. 1970: Sulfide to sulfate reaction mechanism: A study of the sulfide to sulfate reaction mechanism as it relates to the formation of acid mine waters. U.S. Dep. of Inter., Fed. Water Poll. Control Adm., Water Poll. Control. Res. Ser.; FWPCA Grant FPS #14010-FPS-OS-70. Washington, D.C. 115 p.

White, A.F. and S.L. Brantley. 1995. Chemical Weathering Rates of Silicate Minerals, Reviews in Mineralogy Volume 31. Mineralogical Society of America, Washington, D.C. 583 p.

Williamson, M.A. and J.D. Rimstidt. 1994. The kinetics and electrochemical rate-determining step of aqueous pyrite oxidation. Geochim. Cosmochim. Acta, 58. p. 5443-5454. http://dx.doi.org/10.1016/0016-7037(94)90241-0

Appendix Table A1. Particle size distribution with values in percent mass retained. For particles larger than 850 μm, pyrite surface area was negligible.

%S	Particle diameter, μm								
	10-75	75-106	106-150	150-212	212-300	300-500	500-600	600-850	−850
0.04	5.5	1.4	1.9	2.2	2.9	3.5	4.0	6.9	28.3
0.05a	5.8	1.2	1.7	2.1	2.8	3.5	3.8	8.5	29.4
0.05b	6.2	1.2	1.8	2.2	2.9	3.7	4.2	7.2	29.4
0.10	4.9	1.6	2.1	2.5	3.2	4.0	4.5	6.9	29.7
0.12	5.6	1.2	1.8	2.2	2.9	3.7	4.0	8.5	29.9
0.16a	5.1	1.3	2.0	2.3	3.0	3.8	4.0	9.0	30.5
0.16b	6.9	1.5	2.1	2.4	3.3	3.9	4.2	6.7	31.0
0.20	7.2	1.2	1.6	2.1	2.9	3.7	4.4	6.9	30.0
0.26	7.3	1.7	2.2	2.8	3.4	4.8	4.9	7.6	34.7
0.39	7.0	1.2	1.6	1.7	3.2	3.6	4.2	6.7	29.2
0.50	7.9	1.4	1.9	2.4	3.2	4.0	4.4	7.0	32.2
0.59	6.7	1.4	2.0	2.4	3.3	4.0	4.6	7.1	31.5
0.72	5.3	1.0	1.3	1.6	2.1	2.9	3.2	5.3	22.7
1.22	6.3	1.2	1.7	1.5	3.6	3.6	4.0	6.2	28.1
Range	4.9-7.9	1.0-1.7	1.3-2.2	1.5-2.8	2.1-3.6	2.9-4.8	3.2-4.9	5.3-9.0	22-35

Appendix Table A2. Percent sulfur in discrete size fractions. For particles larger than 850 μm, pyrite surface area was negligible.

%S Bulk	Particle diameter, μm								Mass Weighted Mean[1]	Mass Wtd/ Bulk
	10-75	75-106	106-150	150-212	212-300	300-500	500-600	600-850		
0.04	0.06	0.05	0.04	0.04	0.03	0.02	0.02	0.02	0.02	0.50
0.05a	0.07	0.11	0.09	0.08	0.06	0.05	0.07	0.07	0.06	1.20
0.05b	0.05	0.07	0.05	0.06	0.05	0.05	0.04	0.05	0.04	0.80
0.10	0.12	0.11	0.10	0.08	0.08	0.07	0.07	0.07	0.07	0.70
0.12	0.13	0.15	0.10	0.11	0.11	0.09	0.09	0.10	0.10	0.83
0.16a	0.15	0.13	0.12	0.11	0.10	0.11	0.13	0.16	0.13	0.81
0.16b	0.12	0.11	0.11	0.11	0.11	0.11	0.13	0.12	0.12	0.75
0.20	0.39	0.43	0.27	0.17	0.17	0.18	0.18	0.17	0.18	0.90
0.26	0.32	0.28	0.24	0.23	0.21	0.19	0.20	0.22	0.22	0.85
0.39	0.47	0.51	0.51	0.41	0.36	0.33	0.32	0.34	0.37	0.95
0.50	0.65	0.65	0.53	0.53	0.50	0.48	0.49	0.47	0.50	1.00
0.59	0.90	0.66	0.61	0.58	0.59	0.57	0.59	0.61	0.57	0.97
0.72	0.78	0.95	0.97	0.94	0.94	0.82	0.65	0.72	0.65	0.90
1.22	1.16	1.02	0.79	0.72	0.67	0.75	0.81	0.89	1.1	0.90

[1] Determined from masses and sulfur contents of individual size fractions, including fractions larger than 850 μm.

Appendix Table A3. Percent pyrite liberation in discrete size fractions. For particles larger than 850 μm, liberation in all samples was zero.

%S	Particle diameter, μm							
	10-75	75-106	106-150	150-212	212-300	300-500	500-600	600-850
0.04	97	90	77	68	52	0	0	0
0.05a	98	95	90	86	74	0	0	0
0.05b	92	89	67	56	51	46	0	0
0.10	96	91	82	74	45	0	0	0
0.12	96	93	82	57	0	0	0	0
0.16a	98	91	86	73	54	0	0	0
0.16b	99	92	84	73	69	49	43	14
0.20	95	92	78	43	18	11	0	0
0.26	97	83	68	43	26	4	0	0
0.39	95	92	83	75	68	42	33	18
0.50	95	89	84	68	61	53	47	31
0.59	96	91	72	57	22	16	7	0
0.72	94	90	88	82	74	59	8	4
1.22	97	89	89	71	37	8	<5	<5
Range	92-99	83-95	67-90	43-86	0-74	0-59	0-47	0-31

Appendix Table A4. Water retention summary statistics for the greenstone samples.

%S	n[1]	Before leach weight (g)[1]		After leach weight (g)[2]	
		mean	s.d.	mean	s.d.
0.04	204	125	7.0	131	7.1
0.05a	204	144	12.4	148	11.2
0.05b	204	127	5.5	129	5.9
0.10 rep 1	204	130	6.5	140	6.0
0.10 rep 2	154	130	5.5	137	6.0
0.12	204	123	6.6	132	7.3
0.16a	204	134	6.5	140	6.8
0.16b rep 1	204	136	5.6	139	6.8
0.16b rep 2	154	133	6.1	141	6.1
0.20	204	141	7.0	147	8.2
0.26	154	156	4.3	163	5.0
0.39	154	144	8.3	153	8.7
0.50	204	142	7.3	151	7.6
0.59 rep 1	204	125	7.4	134	6.7
0.59 rep 2	154	127	8.1	134	9.2
0.72	204	105	8.4	111	9.0
1.22 rep 1	154	135	7.5	143	8.2
1.22 rep 2	204	146	8.1	151	8.3

[1] before leach: prior to water addition
[2] after leach: 1 day after water added

Appendix Table A5. Average sulfate release rates, exposed pyrite surface areas, and pyrite depletion for the period of record (weeks 20-204 except for 0.26% and 0.39%-S samples which were terminated at week 154).

%S	pH_{med}	dSO_4/dt	$dSO_4/dt \times 0.5$	FeS_2 exposed	FeS_2 depletion
	s.u.	$\mu mol\ (kg\ rock)^{-1}\ wk^{-1}$	$mol\ (kg\ rock)^{-1}\ s^{-1}$	m^2	%
0.04	7.16	3.96	3.28E-12	0.0096	7.2
0.05a	6.90	5.48	4.54E-12	0.013	8.2
0.05b	6.88	4.5	3.73E-12	0.0090	6.4
0.1	6.38	10.1	8.36E-12	0.018	7.1
0.12	6.34	9.42	7.80E-12	0.021	6.2
0.16a	6.38	17.3	1.43E-11	0.023	7.5
0.16b	6.08	13.6	1.13E-11	0.026	6.2
0.2	4.18	57.4	4.75E-11	0.077	5.5
0.26	4.02	91.6	7.58E-11	0.066	27
0.39	4.03	111	9.19E-11	0.096	14
0.50	5.52	102	8.44E-11	0.15	16
0.59	3.35	277	2.29E-10	0.14	31
0.72	7.67	90.2	7.47E-11	0.12	9.2
1.22	3.53	288	2.38E-10	0.21	15